Electronic Supplementary Material (ESI) for Journal of Materials Chemistry A.
This journal is © The Royal Society of Chemistry 2019

Electronic Supplementary Information (ESI)

For

Framework Cu-doped boron nitride nanobelts with enhanced internal electric field for effective Fenton-like removal of organic pollutants

Lingfei Li,[ac] Chun Hu,[b] Lili Zhang,[*a] Guangfei Yu,[ac] Lai Lyu,[b] Fan Li[ac] and Ning Jiang[ac]

[a] Key Laboratory of Drinking Water Science and Technology, Research Center for Eco-Environmental Sciences, Chinese Academy of Sciences, Beijing 100085, China

[b] Key Laboratory for Water Quality and Conservation of the Pearl River Delta, Ministry of Education, Institute of Environmental Research at Greater Bay, Guangzhou University, Guangzhou 510006, China

[c] University of Chinese Academy of Sciences, Beijing 100049, China

* Corresponding author. Tel.: +86 10 62844150; fax: +86 10 62923541.

E-mail address: llzhang@rcees.ac.cn (L. Zhang).

Number of pages: 28

Number of figures: 20

Number of tables: 1

Supplementary Experimental Section:

DFT calculations: Most calculations were performed with the Gaussian 09 program and the B3LYP/6-31+G* (LANL2DZ for Cu) method was used to optimize geometric structures. A structural model containing 42 B atoms and 42 N atoms was used for the basic BN structure, and a Cu-doped BN structure involving 68 B atoms and 68 N atoms was constructed. The ESP distributions were obtained with the VESTA program on the basis of the optimized results. Although the properties estimated with the finite-size model may deviate from those of the real system to some extent owing to size and edge effects, the results obtained from the model could supply a reliable qualitative prediction of the local chemical properties. The Vienna Ab Initio Simulation Package (VASP) for all the adsorption energy calculations within the generalized gradient approximation (GGA) using the PBE functional formulation were used in this work. Projected augmented wave (PAW) pseudopotentials were employed to describe the interactions between ionic cores and valence electrons. 1 (H), 3 (B), 4 (C), 5 (N), and 6 (O) valence electrons were explicitly taken into account. The valence electronic states were expanded in plane wave basis sets with a cutoff energy of 450 eV. Partial occupancies of electronic bands were allowed with the Gaussian smearing method and a width of 0.01 eV. We also adopted the DFT-D3(BJ) method to describe the dispersion effects in the system. The adsorption energy, E_{ads}, of the bisphenol A (BPA) on the optimized structure is calculated as $E_{ads} = E_{M/surf} - E_{surf} - E_M$, where $E_{M/surf}$ and E_{surf} are the total energy of the optimized structure with and without the BPA, respectively, and E_M is the energy of the bisphenol A in

48 vacuum. Based on the above definition, a negative E_{ads} indicates that the adsorption is
49 exothermic and that the adsorbent–BPA system is stable.

50 **Free-radicals quenching:** Several scavenger reagents were introduced into
51 quenching experiments to clarify the active species in the Fenton reaction. During the
52 degradation of BPA (25 mg L^{-1}) in the presence of H_2O_2 (5 mM) in the Cu-BN
53 suspensions (1.0 g L^{-1}), tert-buty lalcohol (TBA, 100 mM) and p-benzoquinone (BQ,
54 1.0 mM) were added into aqueous solution to eliminate the reactive species of $^{\bullet}OH$
55 radicals and $O_2^{\bullet-}$ radicals, respectively.

56 **ESR measurements:** The ESR spectroscopy measurements were conducted as
57 follows: 0.01 g of the prepared powder catalyst was added to 1.0 mL of water or 1.0
58 mL of methanol, followed by the addition of 100 μL of H_2O_2 (30%, w/w) to detect
59 $^{\bullet}OH$ or $O_2^{\bullet-}$, respectively. Subsequently, 90 μL of the above suspension and 5 μL of
60 BMPO (0.25 M) was mixed and held for 5 min, and then the solution was sucked into
61 a capillary. For determining the effect of BPA, 1.0 mL of a high concentration of BPA
62 (100 mg L^{-1}) with water or methanol as solvent was employed to disperse the catalyst.
63 The ESR spectra were recorded on a Bruker A300-10/12 ESR spectrometer using
64 BMPO as a spin trap agent. In the absence of H_2O_2, the ESR signals of the
65 corresponding samples were collected as well.

66 **Measurement for $^{\bullet}OH$ and $O_2^{\bullet-}$ radicals:** The amounts of $^{\bullet}OH$ and $O_2^{\bullet-}$ radicals
67 generated in the reaction process are determined by the terephthalic acid (TPA) probe
68 means[1] and nitroblue tetrazolium (NBT) transformation method[2], respectively. TPA
69 could react with $^{\bullet}OH$ in amolar ratio of 1:1 to generate 2-hydroxyterephthalic acid,

which has strong fluorescence at 425 nm. The fluorescence is recorded on TBS-380 Fluorometer (Turner Biosystems, USA) operating at the excitation wavelength of 310 nm and the emission wavelength of 425 nm. NBT could react with $O_2^{\bullet-}$ in a molar ratio of 1:4 and thus leading to the loss of absorbance at 260 nm. The generated amount of $O_2^{\bullet-}$ can be obtained by monitoring the concentration change of NBT on a U-3900 spectrophotometer (Hitachi, Japan). The conditions of the quantification experiments are consistent with the degradation reaction with the 1.0 g L^{-1} catalyst and 5 mM H_2O_2. The concentrations of TPA and NBT are 50 mM and 0.01 mM, respectively.

Measurement for H_2O_2 utilization efficiency: The calculation of H_2O_2 utilization efficiency (η) was carried out by following equation 1:

$$\eta = [\Delta H_2O_2]_S / [\Delta H_2O_2]_A \quad (1)$$

where $[\Delta H_2O_2]_S$ is the stoichiometric H_2O_2 consumption for the mineralization of BPA according to the equation 2; $[\Delta H_2O_2]_A$ is the actual H_2O_2 consumption at different reaction times, which is measured using a DPD method as previously reported in the literature.[3]

$$C_{15}H_{16}O_2 + 36H_2O_2 \rightarrow 15CO_2 + 44H_2O \quad (2)$$

Supplementary Figures:

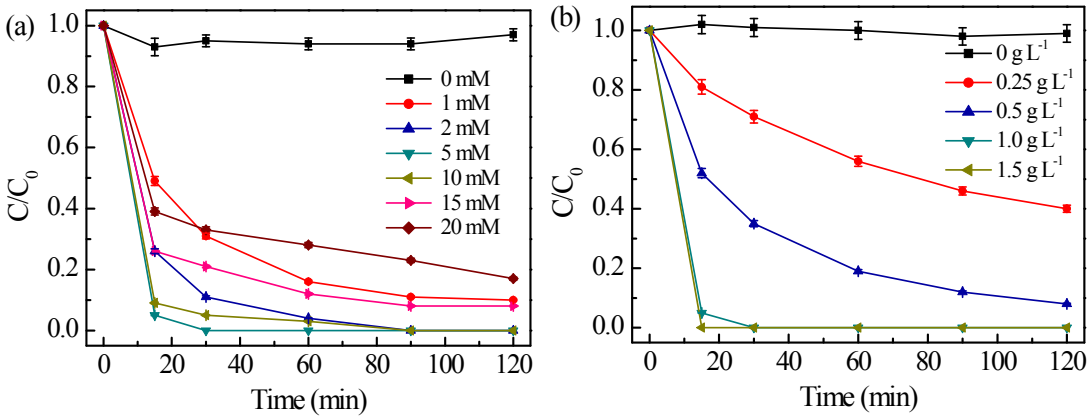

Fig. S1 Effect of (a) H_2O_2 dosage and (b) catalyst concentration on BPA degradation in the Cu-BN reaction system.

The effects of initial H_2O_2 concentration and catalyst concentration on the Fenton catalytic activity in the presence of Cu-BN were investigated. As shown in **Fig. S1a**, in Cu-BN suspension, no significant degradation of BPA was observed in the absence of H_2O_2. On the other hand, the addition of tiny 1 mM H_2O_2 to the BPA suspension lead to a rapid Fenton-like reaction with 90% of BPA degraded within 120 min. The degradation efficiency improved with increasing H_2O_2 concentration, and BPA were degraded completely within 30 min at an optimal H_2O_2 concentration of 5 mM. Nevertheless, the degradation rate decreased using a higher H_2O_2 concentration. Such observations can be ascribed to the reaction between two $^{\bullet}OH$ radicals to produce H_2O_2, as well as an unprofitable consumption from the scavenging effect of H_2O_2, reducing the reactive oxygen species.[4] Moreover, **Fig. S1b** shows the effect of Cu-BN concentration on the catalytic ability in the presence of 5 mM H_2O_2. By increasing the catalyst dosage from 0.25 g L^{-1} to the 0.5 g L^{-1}, the degradation efficiency increased from 60% to 92% within 120 min, respectively, and could reach to 100% at a catalyst

concentration of 1.0 g L^{-1} within 30 min. No significant improvement of the degradation efficiency was exhibited with further increase in the concentration of catalyst. Therefore, the concentrations of 5 mM H_2O_2 and 1.0 g L^{-1} catalyst were selected as the optimal reaction conditions.

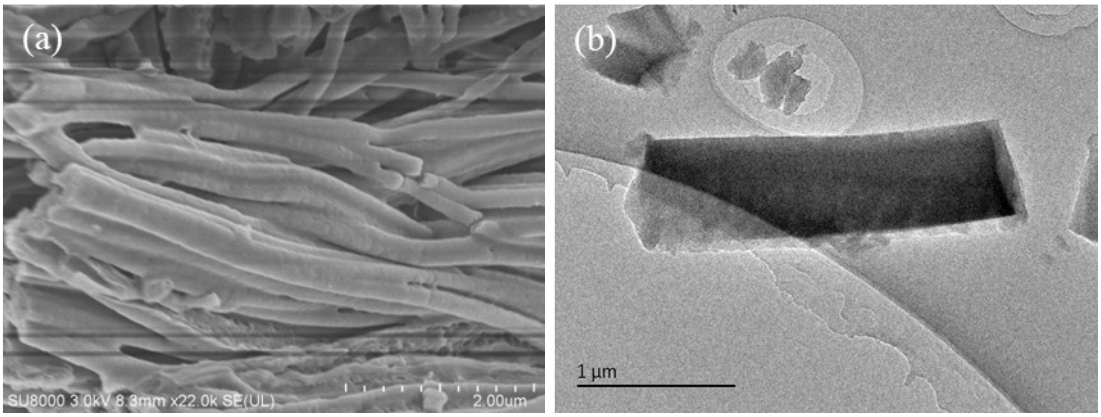

Fig. S2 (a) FESEM image and (b) TEM image of BN.

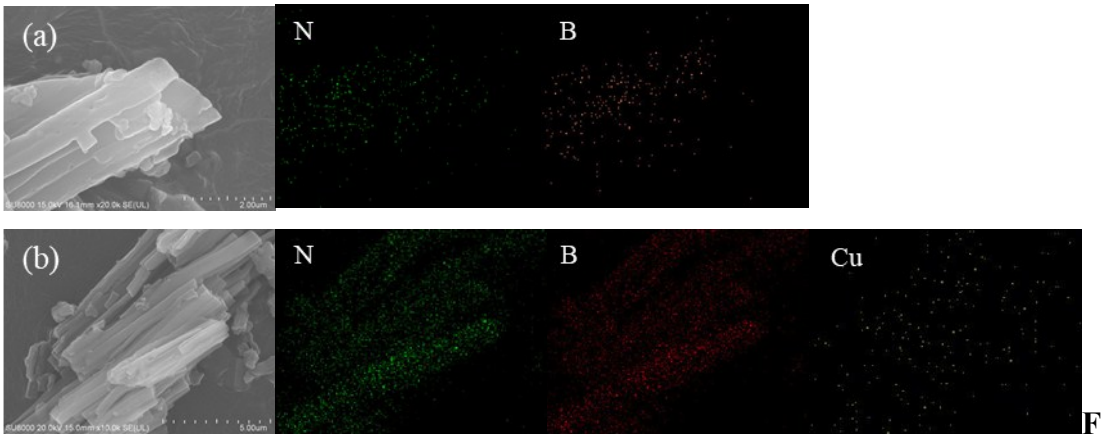

Fig. S3 SEM elemental mapping of (a) BN and (b) Cu-BN.

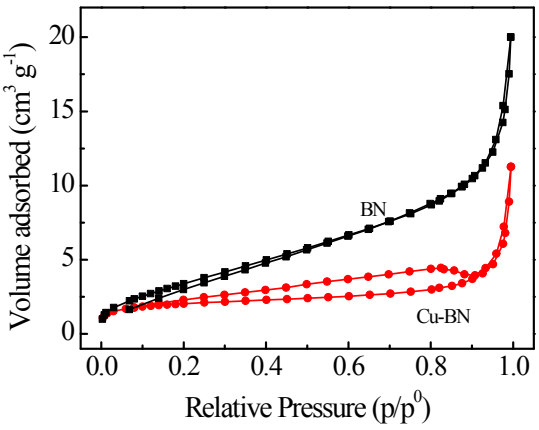

Fig. S4 N_2 adsorption/desorption isotherms of BN and Cu-BN.

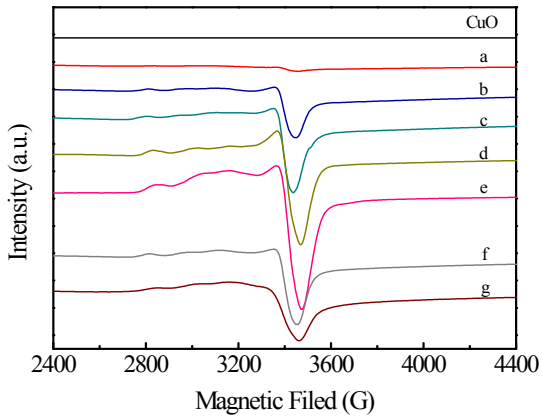

Fig. S5 Solid EPR spectra of the samples, where a-g refer to the catalysts with copper contents of 0, 0.95 wt%, 1.26 wt%, 1.58 wt%, 2.84 wt%, 3.02 wt% and 3.77 wt%, respectively.

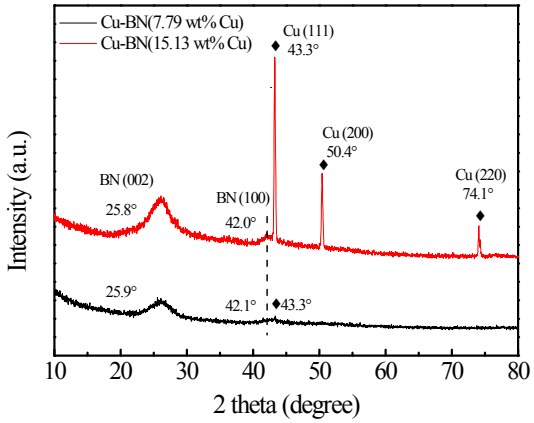

Fig. S6 XRD patterns of the Cu-BN(7.79 wt% Cu) and Cu-BN(15.13 wt% Cu).

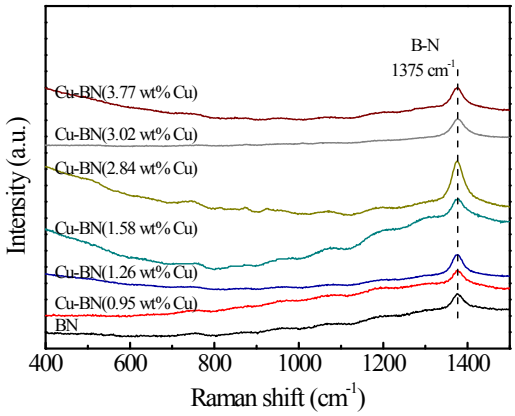

Fig. S7 Raman spectra of the samples.

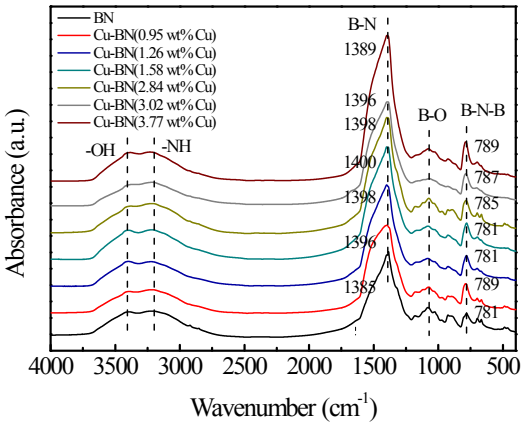

Fig. S8 FTIR spectra of the samples.

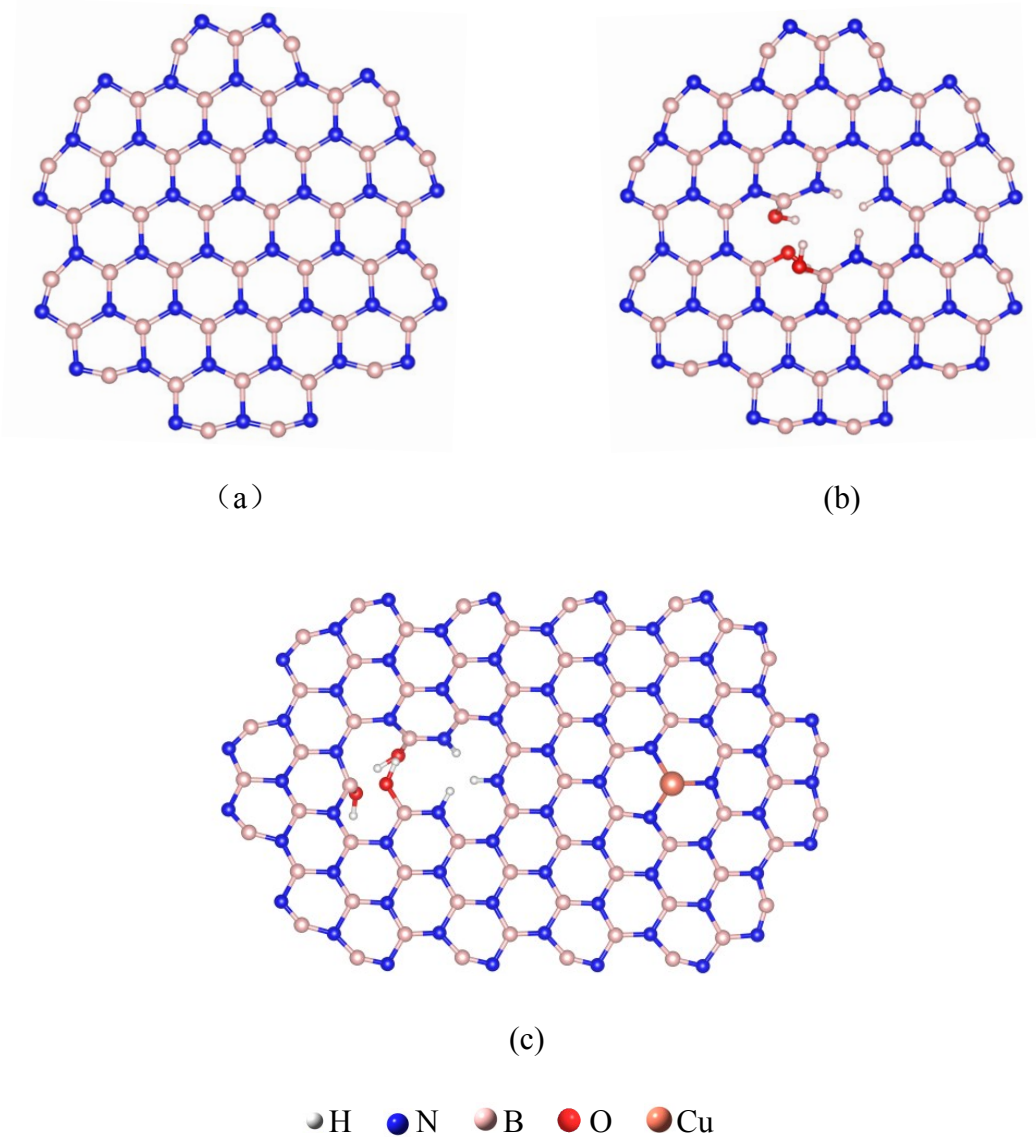

Fig. S9 Structure of (a) perfect BN, (b) as-synthesized BN and (c) Cu-doped BN. (White, blue, pink, red and orange circles denote H, N, B, O and Cu atoms, respectively.)

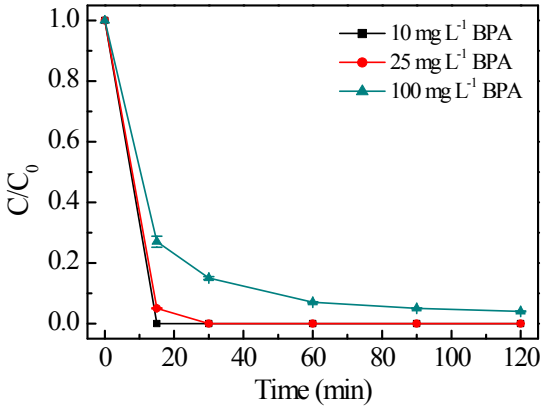

Fig. S10 Effect of initial BPA concentration on degradation in Cu-BN suspensions. (Reaction conditions: initial pH 6.2, initial H_2O_2 concentration 5 mM, catalyst concentration 1.0 g L^{-1}.)

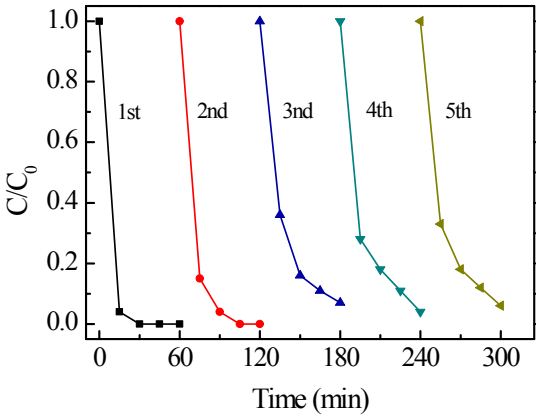

Fig. S11 Reusability of the Cu-BN catalyst for the degradation of BPA. (Reaction conditions: initial pH 6.2, initial BPA concentration 25 mg L^{-1}, initial H_2O_2 concentration 5 mM, catalyst concentration 1.0 g L^{-1}.)

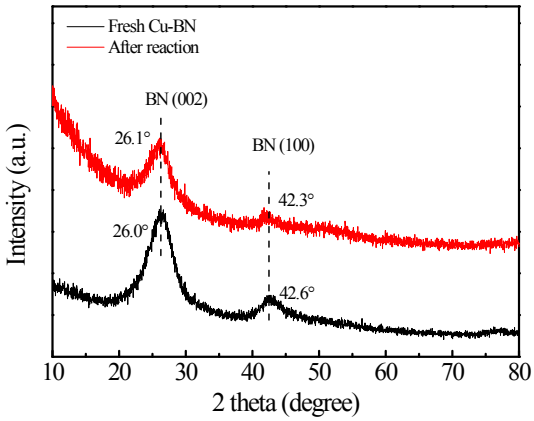

Fig. S12 XRD patterns of the Cu-BN before and after reaction.

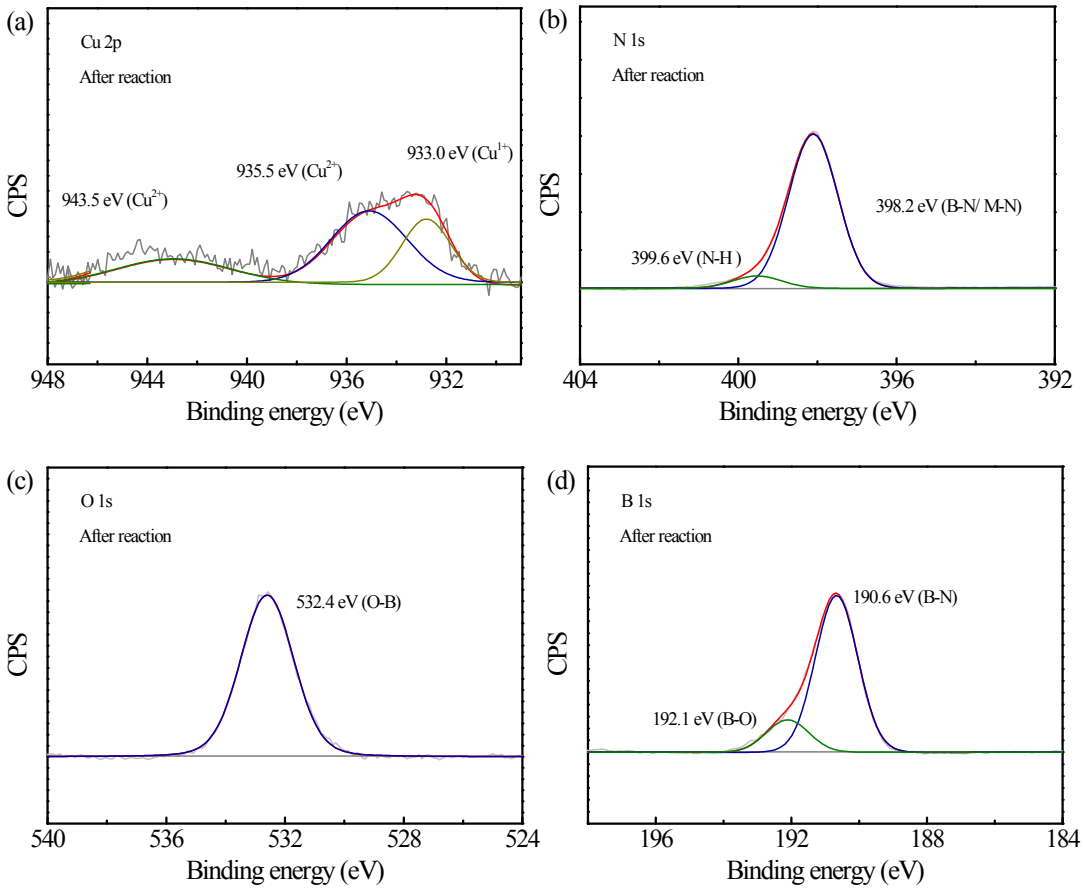

Fig. S13 (a) Cu $2p_{3/2}$ XPS spectra, (b) N 1s XPS spectra, (c) O 1s XPS spectra and (d) B 1s XPS spectra of Cu-BN after reaction.

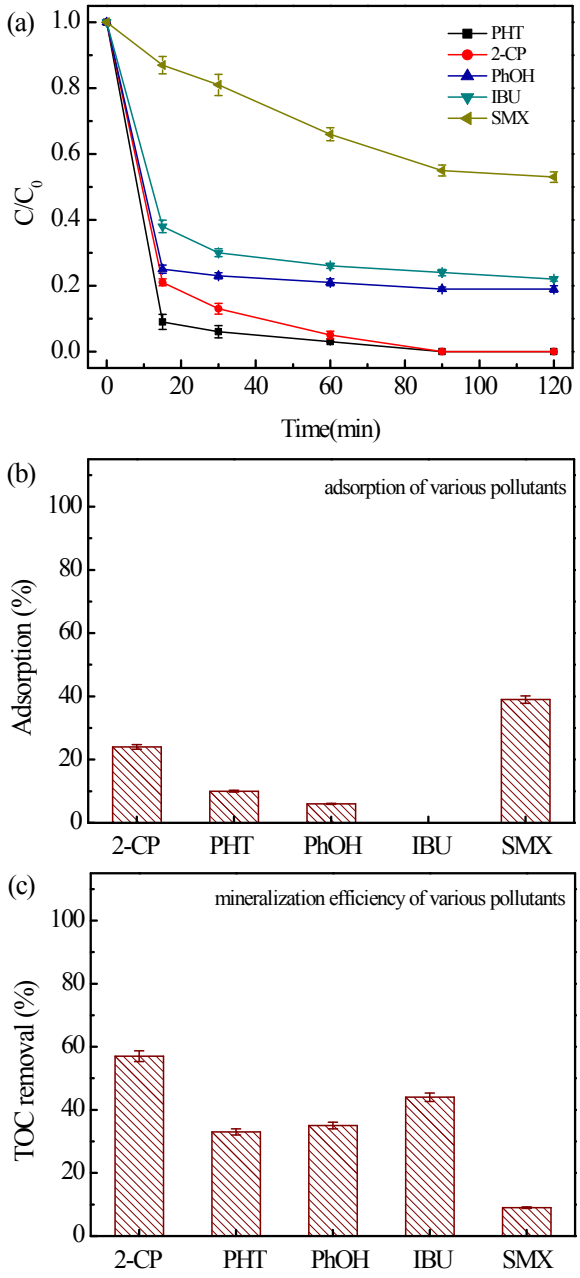

Fig. S14 (a) The degradation of various pollutants in Cu-BN suspensions at natural pH; (b) Adsorption and (c) Mineralization efficiency of various pollutants. (Reaction conditions: initial pollutants concentration 10 mg L^{-1}, initial H_2O_2 concentration 5 mM, catalyst concentration 1.0 g L^{-1}.)

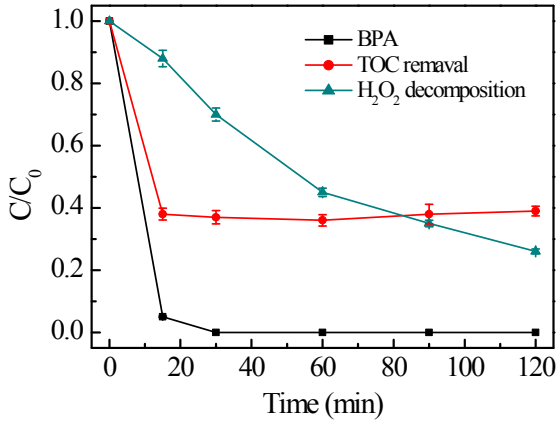

Fig. S15 Decomposition of H_2O_2 in Cu-BN suspension, degradation of BPA and the corresponding TOC removal. (Reaction conditions: initial pH 6.2, initial BPA concentration 25 mg L^{-1}, initial H_2O_2 concentration 5 mM, catalyst concentration 1.0 g L^{-1}.)

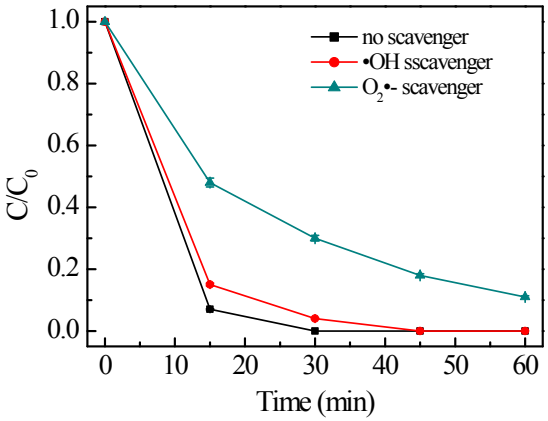

Fig. S16 Effect of different radical scavengers on BPA degradation in Cu-BN suspensions. (Reaction conditions: initial BPA concentration 25 mg L^{-1}, initial H_2O_2 concentration 5 mM, catalyst concentration 1.0 g L^{-1}.)

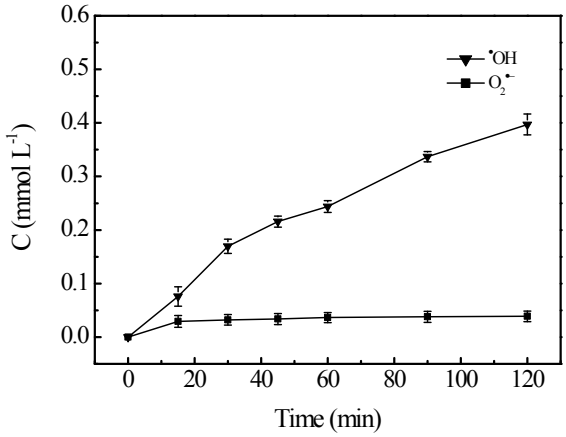

Fig. S17 The concentration of $^{\bullet}OH$ and $O_2^{\bullet-}$ radicals generated in Cu-BN suspensions during the reaction. (Reaction conditions: initial TPA concentration 50 mM, initial NBT concentration 0.01 mM, initial H_2O_2 concentration 5 mM, catalyst concentration 1.0 g L^{-1}.)

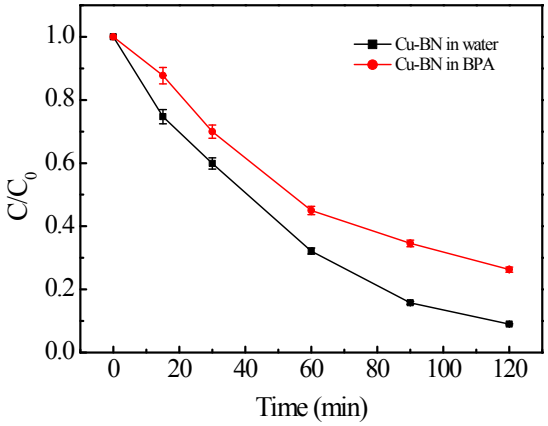

Fig. S18 Effect of different solutions on H_2O_2 decomposition in the Cu-BN suspension under natural pH. (Reaction conditions: initial BPA concentration 25 mg L^{-1}, initial H_2O_2 concentration 5 mM, catalyst concentration 1.0 g L^{-1}.)

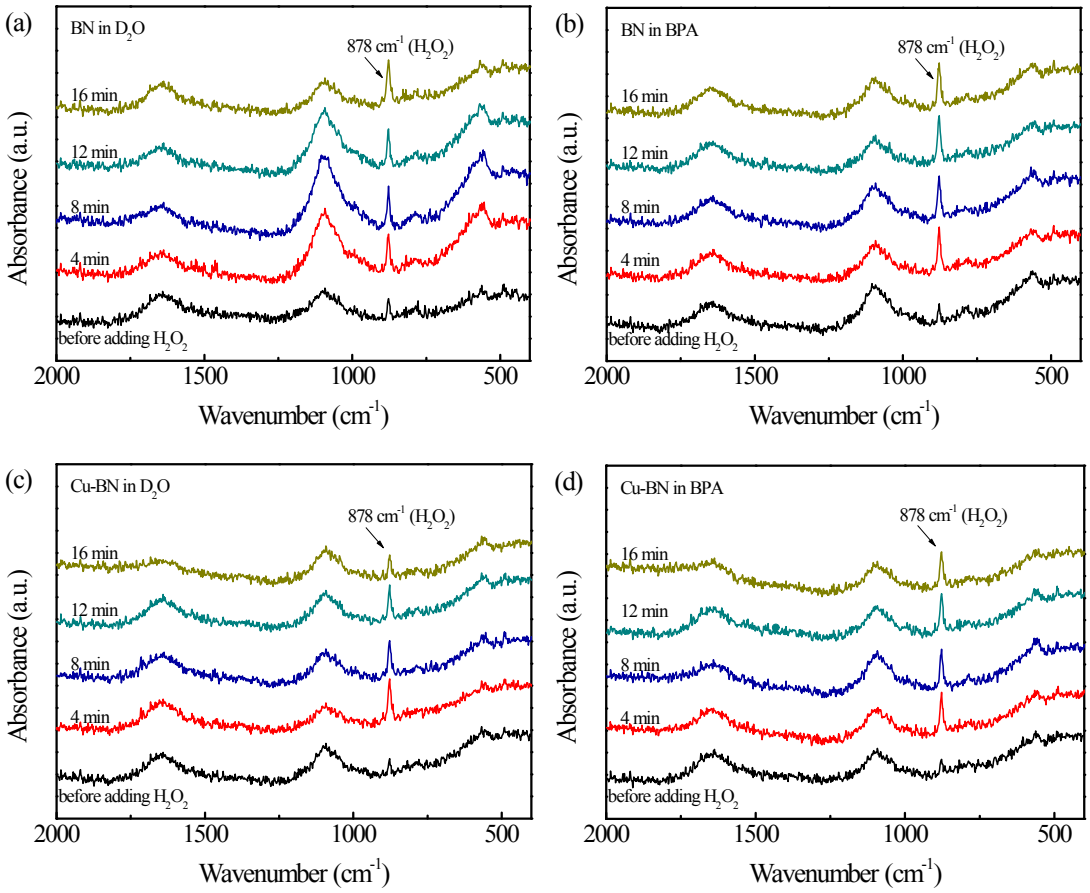

Fig. S19 *In situ* Raman spectra for samples in different dispersions: (a) BN in water dispersions; (b) BN in aqueous dispersions with BPA (100 mg L^{-1}); (c) Cu-BN in water dispersions; (d) Cu-BN in aqueous dispersions with BPA (100 mg L^{-1}).

As shown in **Fig. S15 a and b**, the peak at 878 cm^{-1} attributed to H_2O_2 did not change significantly in the BN suspension whether BPA was present or not, while the peak became weaker with the increase of contact time in the Cu-BN suspension (**Fig. S15 c and d**), indicating H_2O_2 was rapidly decomposed in the Cu-BN suspension. At the same time, the decomposition of H_2O_2 was slower in Cu-BN suspension with BPA, which was consistent with the results of the H_2O_2 decomposition experiment, verifying that BPA and its intermediates could adsorb onto the electropositive Cu sites and prevent the noneffective decomposition of H_2O_2.

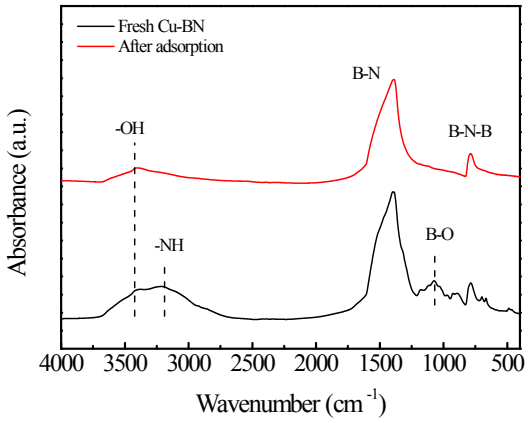

Fig. S20 FTIR spectra of Cu-BN before and after adsorption of BPA.

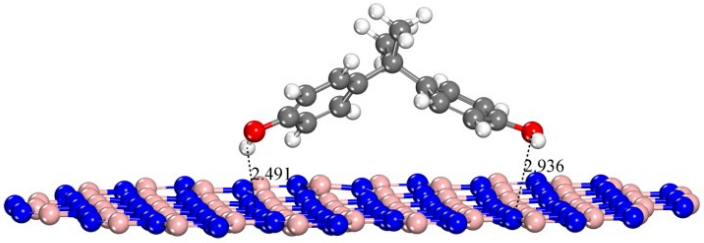

E_{ads} = -0.72 eV

(a)

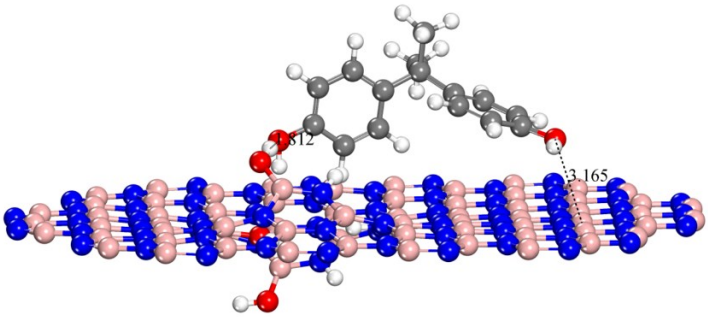

E_{ads} = -1.04 eV

(b)

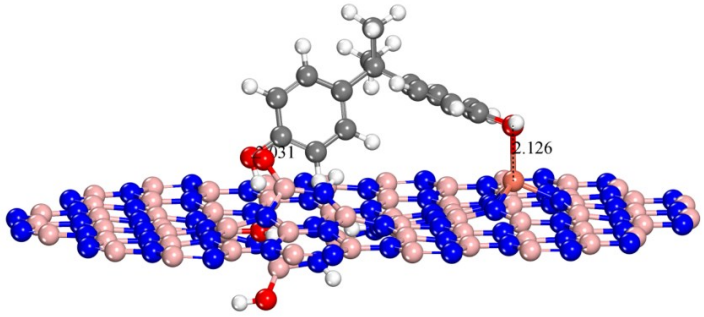

E_{ads} = -1.81 eV

(c)

Fig. S21 Optimized structures of a BPA molecule adsorbed on the (a) perfect BN, (b) as-synthesized BN and (c) Cu-doped BN. (Gray, white, blue, pink, red and orange circles denote C, H, N, B, O and Cu atoms, respectively.)

Table S1 XPS analysis of samples.

Samples	Cu $2p_{3/2}$ Cu^{1+} binding energy (eV)	Cu $2p_{3/2}$ Cu^{2+} binding energy (eV)	B 1s B-N binding energy (eV)	B 1s B-O binding energy (eV)	N 1s N-B binding energy (eV)	N 1s N-H binding energy (eV)
BN	/	/	190.5 (58.4 %)	192.2 (41.6 %)	398.1 (76.9 %)	399.2 (23.1 %)
Cu-BN(0.95 wt% Cu)	933.1 (82.6 %)	936.0 (11.1 %) 946.1 (6.3 %)	190.5 (61.2 %)	192.1 (38.8 %)	398.1 (80.9 %)	398.9 (19.1 %)
Cu-BN(1.26 wt% Cu)	933.0 (59.6 %)	935.4 (12.3 %) 944.0 (28.1 %)	190.5 (61.6 %)	192.0 (38.4%)	398.1 (78.5 %)	399.1 (21.5 %)
Cu-BN(1.58 wt% Cu)	933.1 (20.9 %)	935.6 (30.1 %) 944.0 (49.0 %)	190.6 (63.2 %)	192.3 (36.8%)	398.1 (76.0 %)	399.1 (24.0 %)
Cu-BN(2.84 wt% Cu)	933.3 (16.8 %)	935.3 (54.1 %) 942.9 (29.1 %)	190.4 (63.3 %)	191.8 (36.7%)	398.0 (80.0 %)	398.8 (20.0 %)
Cu-BN(3.02 wt% Cu)	933.0 (12.2 %)	935.3 (54.1 %) 943.2 (33.7 %)	190.5 (57.4 %)	191.9 (42.6 %)	398.1 (80.9 %)	399.1 (19.1 %)
Cu-BN(3.77 wt% Cu)	933.1 (12.7 %)	935.3 (67.8 %) 943.5 (19.5 %)	190.5 (63.6 %)	191.6 (36.4 %)	398.1 (80.3 %)	398.6 (19.7%)
Cu-BN(7.79 wt% Cu)	933.2 (7.8 %)	935.4 (61.7 %) 943.5 (30.5 %)	190.6 (62.9 %)	191.7 (37.1 %)	398.2 (81.3 %)	398.9 (18.7 %)
Cu-BN(15.13 wt% Cu)	933.0 (12.5 %)	935.3 (63.3 %) 943.5 (24.2 %)	190.6 (62.9 %)	191.6 (37.1 %)	398.2 (87.9 %)	399.0 (12.1 %)

References

1. L. Linxiang, Y. Abe, Y. Nagasawa, R. Kudo, N. Usui, K. Imai, T. Mashino, M. Mochizuki and N. Miyata, *Biomed Chromatogr*, 2004, **18**, 470-474.
2. H. Huang, S. Tu, C. Zeng, T. Zhang, A. H. Reshak and Y. Zhang, *Angewandte Chemie-International Edition*, 2017, **56**, 11860-11864.
3. H. Bader, V. Sturzenegger and J. Hoigne, *Water Research*, 1988, **22**, 1109-1115.
4. H. A. Bicalho, J. L. Lopez, I. Binatti, P. F. R. Batista, J. D. Ardisson, R. R. Resende and E. Lorençon, *Molecular Catalysis*, 2017, **435**, 156-165.